



Study of Flutter Behaviors of Plate-like Wings with Stiffeners

Nattawat Chantatul* and Boonchai Watjatrakul

Department of Mechanical and Aerospace Engineering, Faculty of Engineering, King Mongkut's University of Technology North Bangkok, Bangkok, Thailand

*Corresponding author, E-mail: tomtaoname4@gmail.com

Abstract

This paper presents the study of flutter characteristics of isotropic plate-like wings with stiffeners. The analysis model is developed to investigate the interaction between inertial, elastic, and aerodynamic forces. The wing flutter analysis couples the structural model using the Rayleigh-Ritz method and classical plate theory, given the wing mode shapes, with the aerodynamic model using Doublet Lattice Method (DLM), given unsteady aerodynamic loads. The V-g method is employed for the instability analysis. A MATLAB code was developed to implement the proposed analysis. The flutter behaviors of isotropic plate-like wings with geometry variations including the aspect ratio, sweep angle, taper ratio, and thickness are explored. Further, the results of plate-like wings without stiffeners are validated and in good agreement with the benchmark problem available in the literature. The flutter behaviors of plate-like wings with stiffeners are studied.

Keywords: Aeroelastic, divergence, flutter, Aerodynamic loads, Doublet Lattice Method (DLM) and V-g method.

1. Introduction

In this paper, the researchers present the study of the dynamic aeroelastic behaviors of plate-like wings without and with stiffeners. The models considered in this study include the structural dynamic model and the aerodynamic model, in which an analysis is calculated in the equation of motion to solve the aeroelastic model. The structural dynamic behaviors of isotropic plate-like wings using the Rayleigh-Ritz method and classical plate theory are presented. The stiffened isotropic plates were subjected to clamped-free boundary condition. The polynomial displacement function was used to approximate the deformation of the stiffened plate as a whole. The natural frequencies and the results are compared with those obtained from using the finite element program, SolidWorks™. The results are in good agreement between the two approaches for deflection, natural frequencies, and mode shapes predictions. The thorough reviews of the literature on the study of plates were given, for example, a study by (Leissa, 1969). The equivalent stiffened plate concept was introduced and applied to analyze complex wing structures (Giles, 1989; Kapania & Liu, 2000). The aerodynamic theory used in this paper is developed according to the potential flow theory for unsteady compressible potential flow. The governing equation for incompressible steady potential flow is the Laplace's Equation, a linear partial differential equation. In previous work by (Attar, Dowell & White, 2005; Tang, Dowell & Hall, 2006), the Laplace's Equation was employed to solve aerodynamic loads using the VLM. In this dissertation, doublets replace the vortices in the DLM as developed by Rodden in the 1960s work to solve the aerodynamic potential equation (Albano & Rodden, 1969). A computational tool code in MATLAB was developed to explore the analyses of the aerodynamic forces of an isotropic plate-like wing for a steady flow, and results are compared with those obtained from the program, Tornado (Tomas, 2001). The results are in good agreement to calculating the lift distribution on models.

2. Objectives

1. To study of flutter characteristics of plate-like wings from defined variables.
2. To develop a computational tool code in MATLAB for analyzing dynamic aeroelastic.
3. To develop the methodology for predicting the flutter speed to apply with a simple structural wing.

3. Materials and Methods

3.1 The structure dynamic model

The maximum kinetic energy for free transverse vibration of a plate $T_{p,max}$ is shown as follows:



$$T_{p,\max} = \frac{1}{2} h \rho \omega^2 \int_0^{L_x} \int_0^{L_y} (\bar{w}^0)^2 dy dx \quad (1)$$

where h is width of plate, ρ is the material density and ω is circular frequency.

The maximum strain energy of a plate $U_{p,\max}$ is shown as follows:

$$U_{p,\max} = \frac{1}{2} \int_0^{L_x} \int_0^{L_y} \left[D \left(\frac{\partial^2 \bar{w}^0}{\partial x^2} \right)^2 + D \left(\frac{\partial^2 \bar{w}^0}{\partial y^2} \right)^2 + D \left(\frac{2 \partial^2 \bar{w}^0}{\partial x \partial y} \right)^2 \right] dy dx \quad (2)$$

where D is bending stiffness: $\frac{Eh^3}{12(1-\nu^2)}$, ν is Poisson's ratio and E is the modulus of elasticity

The maximum kinetic energy $T_{s,\max}$ and strain energy $U_{s,\max}$ of the stiffener during vibration are obtained as follows:

$$T_{s,\max} = \frac{1}{2} h \rho \omega^2 \int_0^{L_x} \int_0^{L_y} (\bar{w}^0)^2 dy dx \quad (3)$$

$$U_{s,\max} = \frac{1}{2} E_s I_s \int_{L_s} \left(\frac{\partial^2 \bar{w}^0}{\partial x^2} \right)^2 dx \quad (4)$$

where \bar{w}^0 is the deflection amplitude which can be computed as follows:

$$\bar{w}^0(x, y) = \sum_i^m \sum_j^n c_{ij} X_i(\phi) Y_j(\psi) \quad (5)$$

where c_{ij} are unknown coefficients. The trial functions in Eq. (5) can be calculated by using Eq. (6).

$$\begin{aligned} X_j(\phi) &= \phi^{j-1}, Y_j(\psi) = \psi^{j+1}, \\ \phi &= x/a, \psi = y/b \end{aligned} \quad (6)$$

For free vibration analysis, the Rayleigh-Ritz method requires the minimization of the total energy with respect to each of the c_{ij} coefficients (Meirovitch, 1997) as follows:

$$\begin{aligned} \frac{\partial}{\partial c_{ij}} \left[(U_{p,\max} + U_{s,\max}) + (T_{p,\max} + T_{s,\max}) \right] &= 0; \\ i, j &= 1 \dots m, n \end{aligned} \quad (7)$$

Consequently, Eq. (7) leads to an eigenvalue problem as follows:

$$(K - \lambda M)c = 0 \quad (8)$$

where M and K are square $m \times n$ mass and stiffness matrices. The eigenvectors are associated with each eigenvalue. Then, we express the eigenvectors $\lambda^{(\text{mode})}$ and each of the eigenvalues $c^{(\text{mode})}$ as

$$\lambda^{(\text{mode})} = (\omega^2)^{(\text{mode})} \quad (9)$$



$$c^{(mode)} = \begin{Bmatrix} c_1 \\ c_2 \\ \vdots \\ c_{36} \end{Bmatrix}^{(mode)} \quad (10)$$

By substitution coefficients c_{ij} , each of mode shapes into Eq. (5) gives the corresponding mode shapes (Z_a)

of the plate. The natural frequency is then obtained from the eigenvalue as follows: $f_n = \frac{\omega}{2\pi}$ (Hz).

We express the system structural modal as written in Eq. (11).

$$Z_a = \sum_m q_m(t) Z_m(x_c, y_c) \quad (11)$$

Where (Z_a) are mode shapes in Eq. (11) which function polynomial in order ($m = 6, n = 6$) of the deflection amplitude is expanded in Eq. (5). A sixth order polynomial of modeling a mode shape with 36 coefficients is presented. Therefore, since 10 eigenmodes are used in developing the aeroelastic equations, 360 coefficients can be computed as follows:

$$Z_m = \sum_{m=1}^{10} [c_1 y_c^2, c_2 y_c^3, c_3 y_c^4, c_4 y_c^5, c_5 y_c^6, c_6 y_c^7, \dots, c_{36} x_c^5 y_c^7] \quad (12)$$

3.2 The aerodynamic analysis

The Doublet Lattice Method (DLM) (Gulcat, 2010) is based on a linear theory using a numerical approach to study subsonic three-dimensional flow past complex lifting surfaces. Each of doublet line is taken on the box (N_{panel}). Each of the numbers of panels will create a force, f_i . The relation between the normal wash induced at a point (x_i, y_i) by j^{th} doublet line on the surface and the position of the downwash collocation point as shown in Figure 1.

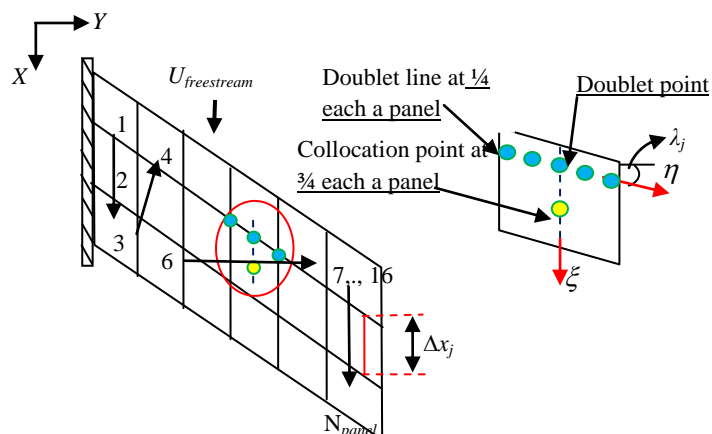


Figure 1 General grid for the Doublet Lattice Method.

The total normal wash caused by the n doublet line at point (x_i, y_i) is the sum of normal washes induced by the number of doublet lines, expressed as follows:



$$w_i(x_i, y_i) = \sum_{j=1}^n \left(\frac{f_j}{4\pi\rho} U_{freestream}^2 \right) \int_{I_j} K[x_i, y_i; x_j(\mu), y_j(\mu)] d\mu \quad (13)$$

Eq. (13) can be written in the matrix-like form as

$$\bar{w}_i = \sum_{j=1}^n D_{ij} \bar{P}_j \quad (14)$$

where

$$D_{ij} = \frac{1}{8\pi} \Delta x_i \cos \lambda_i \int_{I_j} K[x_i, s_i; x_j(\mu), s_j(\mu)] d\mu \quad (15)$$

The area is approximated for the case where the wing is swept by defining the panel average chord Δx_j and sweep angle of the doublet line segment, λ_j . The aerodynamic influence coefficient (AIC) is the inverse matrix of the downwash (D_{ij}) to determine the unknown pressure, as follows:

$$\bar{P}_i = \sum_{j=1}^n AIC_{ij} \bar{w}_j \quad (16)$$

Consequently, Eq. (14) leads to determine the pressure distribution (\bar{P}_i) calculated by the DLM which must satisfy boundary conditions the normal wash (\bar{w}_i) in order that each of the mode shapes with a selection of position at collocation point (x_i, y_i) .

$$\bar{w}_i = \frac{w}{U} = \frac{1}{U} \frac{\partial Z_a(x_c, y_c)}{\partial t} + \frac{\partial Z_a(x_c, y_c)}{\partial x} \quad (17)$$

The original DLM results using a parabolic approximation to determine the kernel function developed by Laschka can be expressed as follows:

$$\sum_{n=1}^{11} a_n e^{-ncu} \quad (18)$$

where $c = 0.372$.

The improve DLM results using a quartic approximation (Rodden, Taylor & McIntosh, 1998) developed by Desmarais can be expressed as follows:

$$\sum_{n=1}^{12} a_n e^{-(2^{n/m})bu} \quad (19)$$

where $m = 1$, $b = 0.009054814793$. Two main integrals for determining the kernel function involved comparisons between the coefficients of Laschka (Parabolic Approx.) and coefficients of Desmarais (Quartic Approx.) are shown in Table 1.



Table 1 Coefficients Laschka and Desmarais Approx.

Parabolic Approx.		Quartic Approx.	
n	a_n	n	a_n
1	0.24186198	1	0.000319759140
2	-2.7918027	2	-0.000055461471
3	24.991079	3	0.002726074362
4	-111.59196	4	0.005749551566
5	271.43549	5	0.031455895072
6	-305.75288	6	0.106031126212
7	-41.183630	7	0.406838011567
8	545.98537	8	0.798112357155
9	-644.78155	9	-0.417749229098
10	328.72755	10	0.077480713894
11	-64.279511	11	-0.012677284771
		12	0.001787032960

3.3 The V-g method

The V-g method in conjunction with the aeroelastic system derived in Eq. (20) is suitable for determining the flutter boundary. The V-g method is an interactive eigenvalue analysis that is based upon choosing the reduced frequency (k), used in calculating the aerodynamics.

The equation of motion for aeroelastic model becomes

$$\sum_m M_{mi} \ddot{q}_m + K_{mi} \dot{q}_m = \frac{\rho U^2}{2} \sum_m A_{mi}(k) q_m \equiv Q_i \quad (20)$$

The modal mass matrix M_{mi} , are square diagonal matrix dimension $N_{(mode)} \times N_{(mode)}$ is given by

$$M_{mi} = \phi^T M \phi \quad (21)$$

where ϕ is a matrix containing a given normalize mode shapes are $M_{N_{panel}} \times N_{(mode)}$ for “Npanel” are number of panels and $N_{(mode)}$ are number of mode shapes.

The modal stiffness matrix K_{mi} , are square diagonal matrix dimension $N_{(mode)} \times N_{(mode)}$ is given by

$$K_{mi} = \omega^2 M_{mi} \quad (22)$$

where ω is the natural frequency is then obtained from eigenvalue.

The aerodynamic influence coefficient matrix, A_{mi} (AICM) are square $M_{N_{panel}} \times M_{N_{panel}}$ matrix, Q_i is the generalized forces from the aerodynamic model. The reduced frequency (k) that is a non-dimensional parameter can be expressed as given

$$k = \frac{\omega b}{U} \quad (23)$$

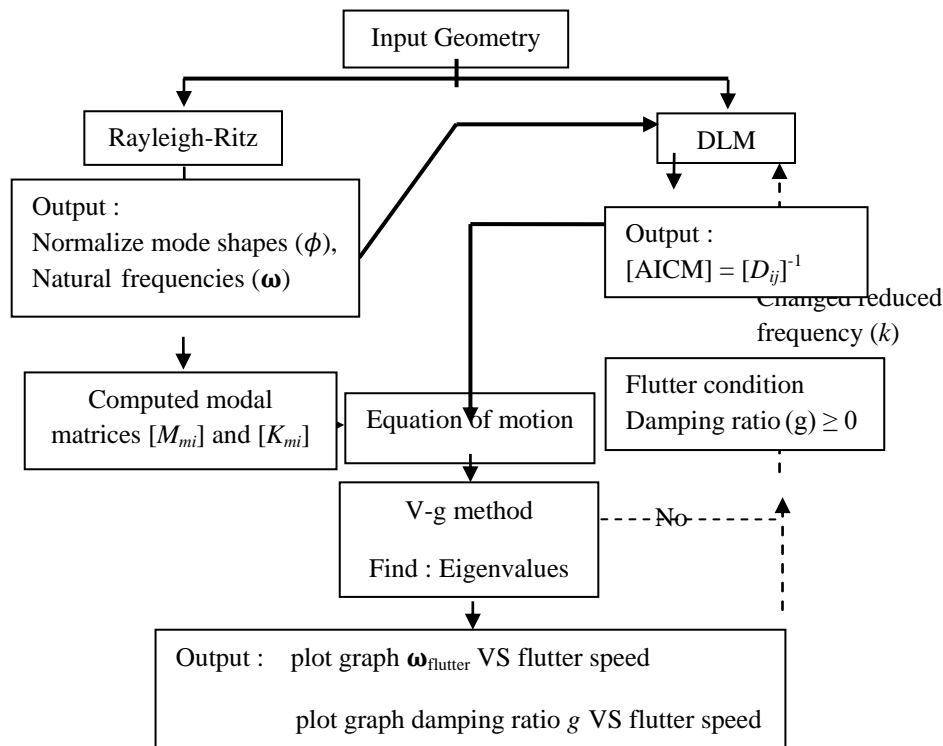
where b is semi-chord and U is flow velocity.

Consequently, Eq. (21) leads to an eigenvalue problem.

$$\left\{ -[M] + \frac{1+ig}{\omega^2} [K] - \frac{\rho b^2}{2k^2} [A(k)] \right\} \{ \bar{q} \} = 0 \quad (24)$$



The eigenvalue $\lambda = \frac{(1+ig)}{\omega^2}$ are computed at every k , and are calculated at each iteration. Its algorithm is shown in Figure 2 where g is the damping ratio.



3.5 Model validation

The present study validates the proposed model by considering 3 cases 1) free vibration analysis case, 2) steady aerodynamic analysis case, and 3) unsteady aerodynamic analysis case. In the first case, the results obtained from the Rayleigh-Ritz method are validated with the results obtained from the program, SolidWorks™. For the second case, the comparisons have been performed between the results from the quartic approximation, the parabolic approximation, and the commercial program, Tornado. Finally, the last case comparisons have been performed between the results from the quartic approximation and those from the reference (Albano & Rodden, 1969). The geometry platform dimensions are shown in Figure 3.

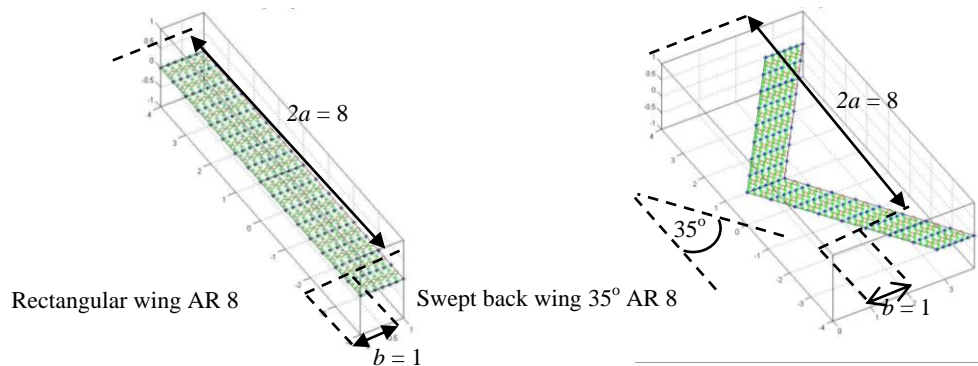


Figure 3 Unswept and swept 35 degree of rectangular plate-like wings.

4. Results and Discussion

4.1 Free vibration analysis

This model used a rectangular wing as shown in Figure 3 (left). The material has an elasticity modulus (E) of 73.8 GPa and density of the material of 2768 kg/m³. The mode shapes obtained from the Rayleigh-Ritz method are compared with those obtained from SolidWorks™ as shown in Figure 4 with 1-mm thickness.

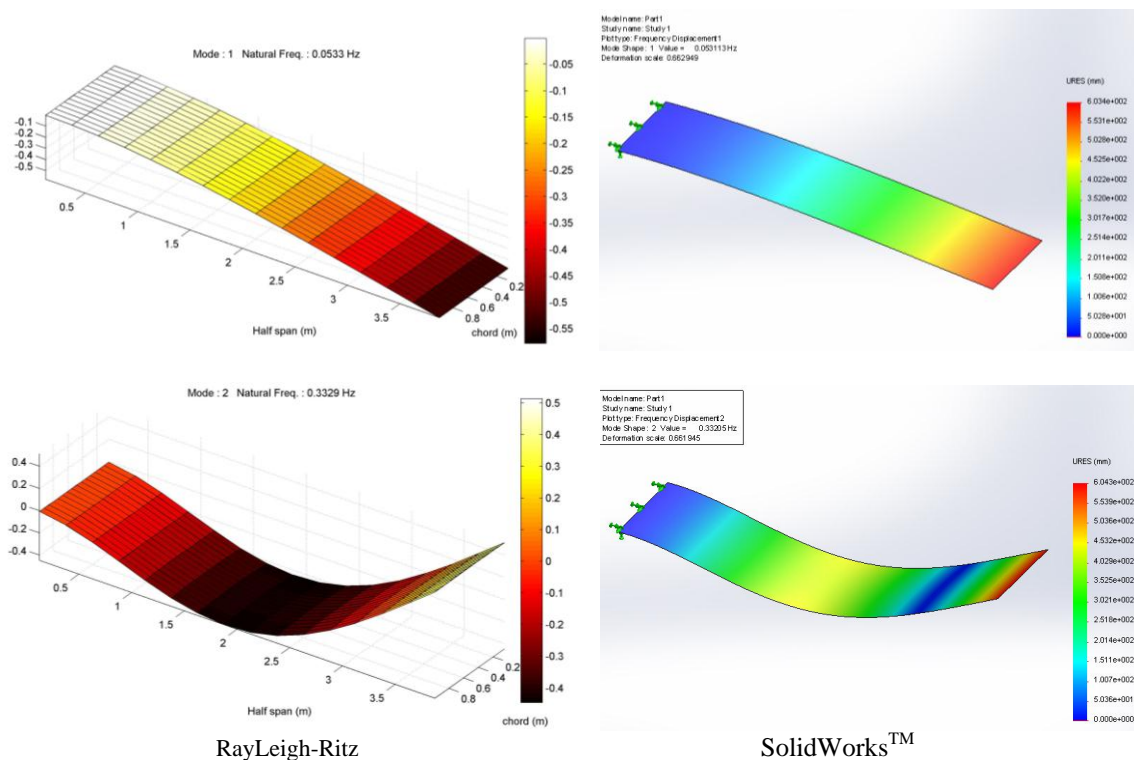


Figure 4 The validation in bending modes of rectangular wing AR 8.



Table 2 Natural frequency of rectangular wing AR 8

No.	Natural Frequency [Hz]		Description	% Error
	Rayleigh-Ritz	SolidWorks™		
1	0.0533	0.0531	1 st Bending mode	0.38
2	0.3329	0.3321	2 nd Bending mode	0.24
3	0.4239	0.4221	1 st Torsion mode	0.43
4	0.9347	0.9325	3 rd Bending mode	0.24
5	1.3099	1.3046	2 nd Torsion mode	0.41

4.2 Steady aerodynamic analysis

The models considered in this study include the steady aerodynamic of a rectangular and sweptback wing with an aspect ratio (AR = 8). The span is divided into 16 strips. A chord is divided into 8 strips as shown in Figure 3. The model with a total of 128 panels are selected to investigate. The steady aerodynamic analysis is chosen the reduced frequency (k) of 0. Figure 5-6 show the validation of the lift coefficient of the proposed model comparison between the quartic approximation (yellow line) with the parabolic approximation (orange line) and with tornado program (blue line).

The rectangular wing was validated with the results. At a Mach number of 0.6 and angle of attack (AOA = 10 degrees), the lift coefficient is shown in Figure 5.

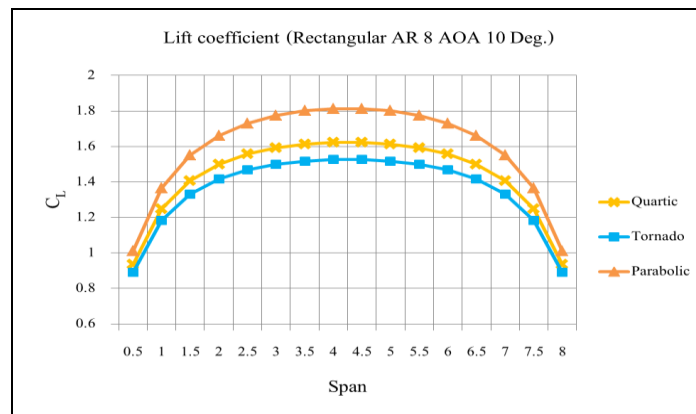


Figure 5 Lift coefficient distribution on rectangular wing Mach 0.6, AR 8 and angle of attack (AOA) 10°.

The sweptback wing is the second case for comparing the results, given Mach number of 0.8 and angle of attack (AOA) of 8 degrees. Results are shown in Figure 6.

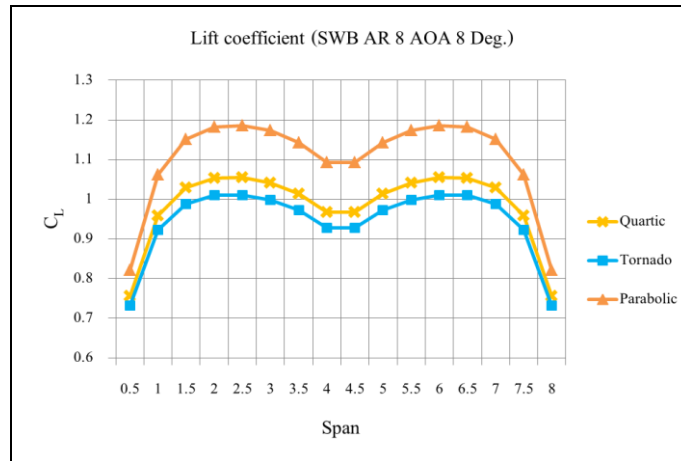


Figure 6 Lift coefficient distribution on SWB wing Mach 0.8, AR 8 and angle of attack (AOA) 8°.

4.3 Unsteady aerodynamic analysis

This present model uses a rectangular wing an aspect ratio (AR = 3) for validating this case as shown in Figure 7. Oscillating in a bending mode described approximately were obtained form

$$h \approx 0.18043 \left(\frac{y}{s} \right) + 1.70255 \left(\frac{y}{s} \right)^2 - 1.13688 \left(\frac{y}{s} \right)^3 + 0.25387 \left(\frac{y}{s} \right)^4 \quad (25)$$

where \bar{h} is the non-dimensional deflection amplitude and α_h is the magnitude of the effect oscillatory angle of attack at the wing tip due to bending. The results are shown in Figure 8. The quartic approximation is validated with the results from Rodden's paper in 1969 (Albano & Rodden, 1969).

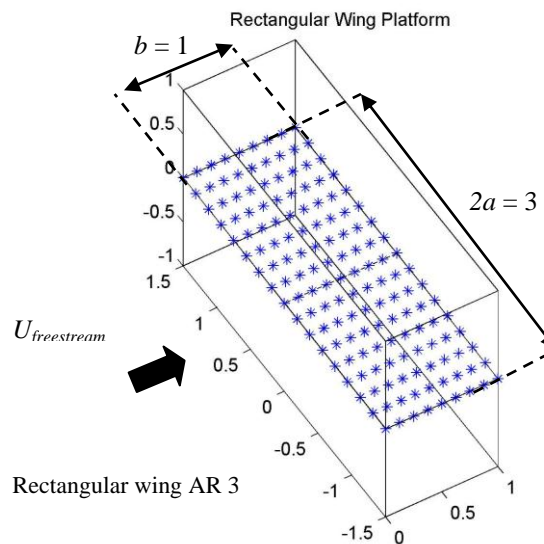


Figure 7 General grid for rectangular wing AR 3.

The pressure coefficient compared in the unsteady aerodynamic analysis has chosen the reduced frequency (k) of 0.47. As shown in Figure 8, the validation of the pressure coefficient of the proposed model with the quartic approximation (blue dashed line) with the experimental results (red square).

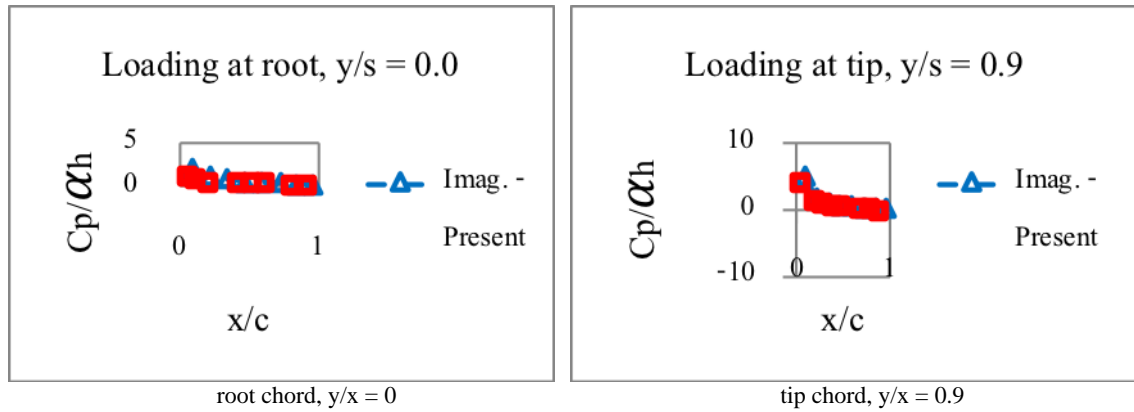


Figure 8 The pressure coefficient distribution on model oscillating in bending mode Mach 0.24, AR 3 and $k = 0.47$.

4.4 Aeroelastic model

This paper presents the models for studying aeroelastic of plate-like wings made of isotropic material properties, as shown in Table 3. Two-case comparisons have been performed between the results obtained 1) without stiffeners and 2) with stiffeners.

Table 3 Properties of an isotropic material.

Plate material properties : Plexiglas (Pl)		
Modulus of Elasticity (E)	(GPa)	2.4
Density of material	(kg/m^3)	1217
Poisson's ratio	(-)	0.33
Plate thickness	(mm)	1.588
Stiffener material properties : Plexiglas		
Cross section ($h \times t$)	(mm^2)	5×1.588
Modulus of Elasticity (E)	(GPa)	2.4
Density of material	(kg/m^3)	1217

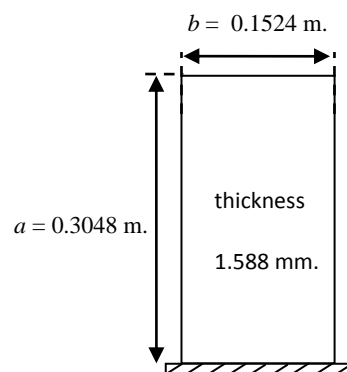


Figure 9 Dimensional drawing of rectangular plate-like wing AR 2.

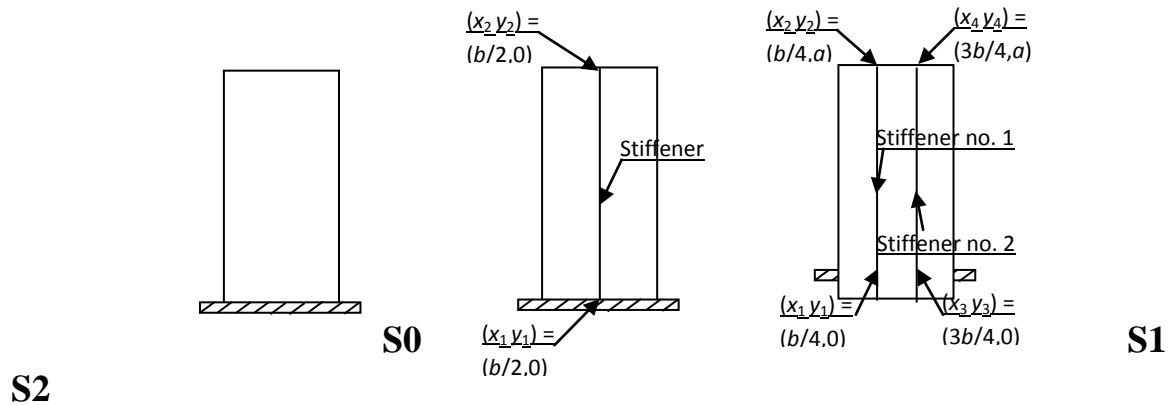


Figure 10 Modeling the stiffeners on rectangular plate-like wing.

The model PI-S0. The model has the geometry as described in Figure 9 with a thickness of 1.588 mm. Material properties are given in Table 3. The result obtained by our present code (row 1) to flutter is at $U_{flutter} = 20.22$ m/s while the experiment results in a flutter speed at 20.05 m/s. The difference between the results of our present code compared with that of the experiment to flutter point is at 0.85%. Meanwhile, the result obtained from the method in the paper has computed the flutter speed of 20.8 m/s. The difference in the results between our present code with that obtained from the paper's method to flutter point is at 2.79%. Furthermore, the flutter mode is specified with the first torsion mode (second natural mode). The results of the damping ratio (g) and flutter frequency of 0.01941 and 9.84 Hz versus flow velocity until the onset of flutter at 20.22 m/s are shown in Figure 11.

Table 4 The flutter speed versus isotropic plate-like wings without stiffeners.

Model	Flutter speed [m/s]				
	Present code	Reference (Howard, 2009)		% Error paper	% Error Exp.
		Paper	Experiment		
PI-S0	20.22	20.8	20.05	2.79	0.85

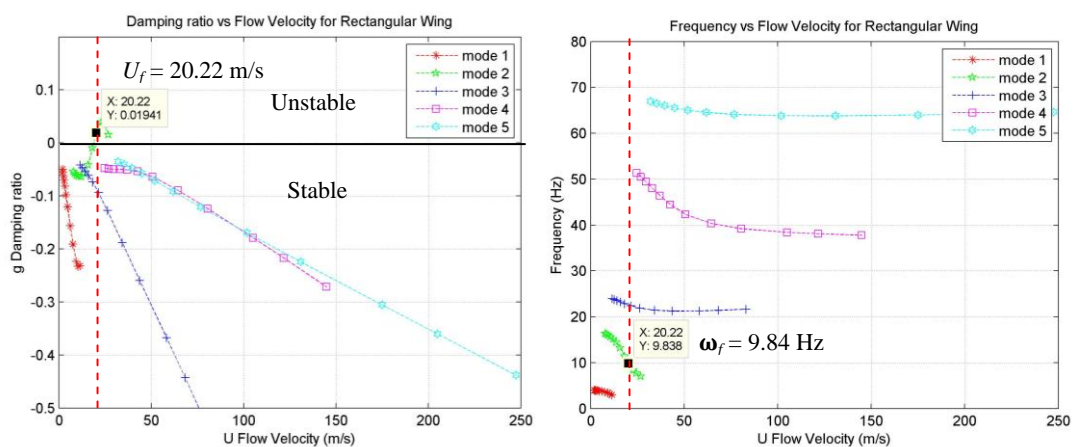


Figure 11 Damping ratio and mode frequency vs flow velocity for the model PI-S0.



The model PI-S1 with added stiffener is shown in Figure 10 (middle). The stiffener material with the same properties as the model is given in Table 3. The positions of stiffener are given at the point $(x_1 = 0.0762)$, $(y_1 = 0)$ and the end point $(x_2 = 0.0762)$, $(y_2 = 0.3048)$. The results are shown in Table 5. The results obtained by our present code predict that the flutter speed occurs at $U_{flutter} = 20.32$ m/s. The flutter is specified with the first torsion mode (the second elastic mode) as shown in Figure 12. The results occur at the damping ratio (g) of 0.00454 versus the flow velocity until onset the flutter speed and the flutter frequency occurs at 10.61 Hz.

The model PI-S2 with added stiffened on plate is shown in Figure 10 (right). The positions of stiffener no. 1 are at the point $(x_1 = 0.0381)$, $(y_1 = 0)$ and the end point $(x_2 = 0.0381)$, $(y_2 = 0.3048)$. The stiffener no. 2 is at the point $(x_3 = 0.1143)$, $(y_3 = 0)$ and the end point $(x_4 = 0.1143)$, $(y_4 = 0.3048)$. For the model and stiffener material with the same properties, the results obtained by our present code predict that the flutter speed occurs at $U_{flutter} = 22.46$ m/s. Figure 13 shows the first five mode shapes. The flutter occurs in the second elastic mode (torsion mode) at the damping ratio ($g = 0.00306$) and the flutter frequency at 10.93 Hz.

Table 5 The results to validated flutter speed between case without stiffeners and with case with stiffeners.

Model	Flutter speed [m/s]			Flutter frequency [Hz]		
	Added 2 Stiffener (S2)	Added 1 Stiffener (S1)	No Stiffener (S0)	Added 2 Stiffener (S2)	Added 1 Stiffener (S1)	No Stiffener (S0)
PI	22.46	20.32	20.22	10.93	10.61	9.84

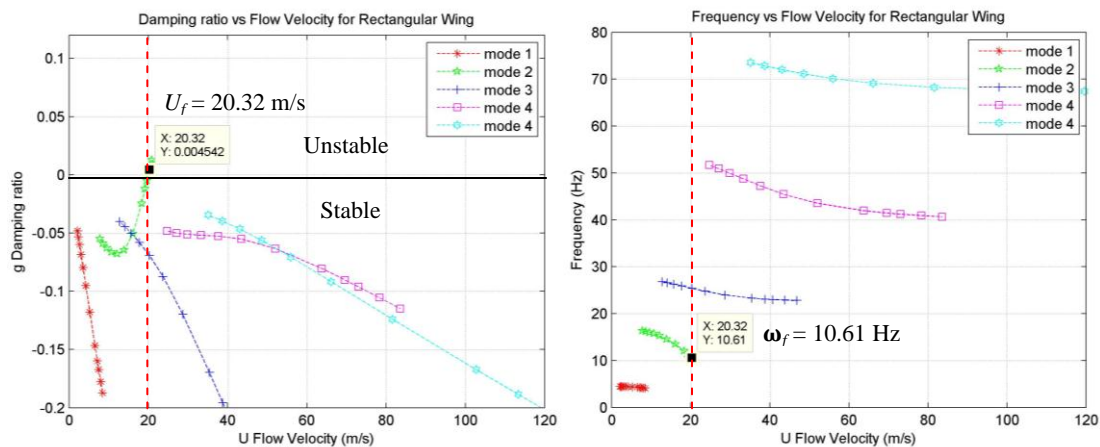


Figure 12 Damping ratio and mode frequency vs flow velocity for the model PI-S1.

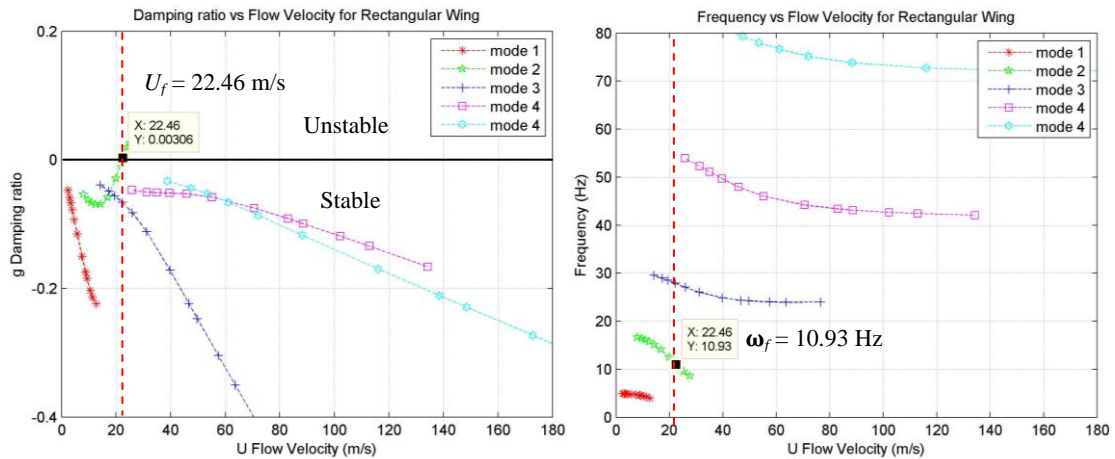


Figure 13 Damping ratio and mode frequency vs flow velocity for the model PI-S2.

5. Conclusion

In this study, an analytical investigation was proposed to determine the aeroelastic model of plate-like wings with stiffeners. The Rayleigh-Ritz method was used to solve a free vibration of the structural dynamic behavior combined with the Doublet Lattice Method which was used to solve the unsteady subsonic flow. Also, the normal wash matrix was used to connect between the aerodynamic points (collocation point on each panel) and structure points. The flutter speeds and flutter frequencies are obtained through the V-g method, and the results are compared to the publications in the literature. This present paper has shown a good agreement in flutter prediction.

A free vibration for validating the results are obtained using the Rayleigh-Ritz method, which well agreed with those obtained from the SolidWorks™.

An analytical: The aerodynamic loads in the steady flow case for validating the lift coefficients distributed over the rectangular and sweptback 35 degrees wing. Based on the program Tornado to refer the lift coefficients distribution, it is concluded that the results obtained through the quartic approximation (improve DLM) are more accurate than those from the parabolic approximation (original DLM). In the unsteady flow case, a comparison between the results of the quartic approximation and the experimental results for validating the pressure coefficients is in good validation.

A linear aeroelastic for studying the effect of flutter speeds and flutter frequencies of plate-like wings with stiffeners was simulated by cantilevered isotropic plate using the V-g method. An analytical investigation was divided into 2 cases; 1) the model without stiffener and 2) the model modified with stiffeners. The improved DLM was used to solve the unsteady aerodynamic analysis. In the first case, the results obtained from our present method are compared with those obtained from the publications in the literature. The V-g method used to solve the compared results has shown the different percentage of the error in the range from 0.85 to 2.79%. In the second case, the models are modified with stiffeners to determine the flutter speeds and flutter frequencies. For validating the results of all cases, it is assumed that flutter points occurred in the torsion mode (twists at the wingtip). Regarding the model modified with 2 stiffeners, an increase in the flutter speed and flutter frequency is shown because this model decreases the twists more than the model modified with 1 stiffener, which affects better the model stability characteristic.

6. Acknowledgements

The author would like to gratefully acknowledge the support of Engineering Faculty, King Mongkut's University of Technology North Bangkok on this study through the research grant.



7. References

- Leissa, A.W. (1969). *Vibration of plates: NASA SP-160*. Washington DC: NASA.
- Giles, G.L. (1989). Further generalization of an equivalent plate representation for aircraft structural analysis. *Journal of Aircraft*, 26(1), 67-74.
- Kapania, R.K., & Liu, Y. (2000). Static and vibration analyses of general wing structures using equivalent-plate models. *AIAA Journal*, 38(7).
- Attar, P.J., Dowell, E.H., & White, J.R. (2005). Modeling the LCO of a delta wing using a high fidelity structural model. *Journal of Aircraft*, 45(2), 1209-1217.
- Tang, D.M., Dowell, E.H., & Hall, K.C. (2006). Limit cycle oscillations of a cantilevered wing in low subsonic flow. *AIAA Journal*, 37(3), 364-371.
- Albano, E., & Rodden, W.P. (1969). A doublet-lattice method for calculating lift distributions on oscillating surfaces in subsonic flows. *AIAA Journal*, 7(2), 279-285.
- Tomas, M. (2001). *Tornado user's guide: Reference manual Tornado*. 1(2.3).
- Meirovitch, L. (1997). *Principles and techniques of vibrations*. New Jersey: Prentice-Hall, Inc.
- Gulcat, U. (2010). *Fundamentals of modern unsteady aerodynamic*. London: Springer.
- Rodden, W.P., Taylor, P.F., & McIntosh Jr., S.C. (1998). Further refinement of the subsonic doublet-lattice lifting surface method. *Journal of Aircraft*, 35(5), 720-727.
- Howard, J.C. (2009). *The effect of wing damage on aeroelastic behavior*. A thesis for the degree of Master of Science. Duke University.